

## Vortex Creation and Pinning in High Amplitude Third Sound Waves

C. Wilson and F. M. Ellis

Department of Physics, Wesleyan University, Middletown, CT 06459

*Changes of macroscopic circulation induced by high amplitude, rotationally polarized waves in a third sound resonator are measured. The results are compared to a model including a simple frictional vortex drag with the substrate. A significantly larger than expected concentration of vorticity is deposited in the vicinity of a central hole piercing the resonator which other modifications to the model cannot address.*

### 1. INTRODUCTION

High amplitude third sound waves excited in a circular resonator can induce a circulatory flow of the film supporting the resonance.<sup>1</sup> Unlike the similar process which swirls a classical fluid, the quantum fluid can only change its circulation through the creation and movement of quantized vortices. As a consequence, the quantum swirling process is an enlightening probe of the properties of vortices in films at low temperatures. In this paper, we compare experimental measurements of the swirling effect in films to numerical simulations based on some simple models for the vortex motion.

A closer comparison of the classical and quantum mechanism for inducing DC flow will first be useful. It will be sufficient to consider the plane wave case for this discussion. As a traveling plane wave propagates forward in a thin fluid layer, a linearized description of the motion has the film flowing forward under the crests and backwards under the troughs of the height oscillations. The flow field is oscillatory everywhere and there is no net motion of any fluid. Classical induced flow is therefore a nonlinear effect and a quantitative description is quite involved.<sup>2</sup> It is not hard, however, to see where it comes from by considering nonlinear quantities derived from the linear solutions. For example, if one includes the linearized results for the height oscillations in addition to the oscillatory flow field, there is a slightly thicker (thinner) film over the wave crests (troughs) where the fluid is moving forward (backward). This

results in a net fluid flux in the forward direction proportional to the square of the wave amplitude  $\eta$  compared to the fluid depth,  $h$ .  $C_3$  is the wave speed.

$$v_{\text{drift}} = \frac{1}{2} C_3 \left( \frac{\eta}{h} \right)^2 \quad (1)$$

Now consider the quantum fluid picture. In order to create a forward DC flow, there must be a polarization of vortices resulting in more left handed vortices to the right, and more right handed vortices to the left of the forward direction. The vortices could be polarized from an initially random distribution of left and right species or polarized after a left-right nucleation event. In the absence of any DC flow, if the arguments leading to (1) are to result in zero drift, the backflow under the wave troughs must be slightly larger than the forward flow under the crests. Within such a flow, vortices with any kind of drag interaction with the substrate or normal fluid will be herded by "Magnus forces" the appropriate direction to increase the flow forward. Thus, in order to create a flow, vortices must be nucleated (in pairs) if they are not already present in the film, and must experience some sort of dissipative drag if they are to be subsequently polarized.

The qualitative consequences of the classical-quantum fluid comparison are as follows. Within a traveling wave, classical DC drifts will increase gradually (quadratically) with amplitude and return to zero through dissipation after the wave motion ends. In the quantum fluid traveling wave, there is a threshold amplitude for creating vorticity (nucleation) or overcoming drag effects (pinning), or both. Above this amplitude, polarization occurs, creating a flow. If the wave amplitude is decreased to zero, the same drag effects pin the vortices in the polarized state and the flow remains as a persistent current.

## 2. EXPERIMENT

The above qualitative features of quantum drift have been observed as swirling induced by rotating waves in a third sound resonator. The third sound is resonated in a superfluid film adsorbed on the inner surfaces of a flat, circular cavity formed between two gold plated microscope slides. The perimeter is defined by epoxy which fills the gap for radii larger than  $a=6.15\text{mm}$  and holds the gap at  $8\mu\text{m}$ . Electrically isolated regions of the gold coating serve as capacitive transducers which couple to the weakly dielectric helium film. Two drive regions at a  $90^\circ$  angular orientation allow circularly polarized drive forces to act on odd  $m$  modes. A single pickup region is incorporated as the capacitor of a 77Mz L-C tunnel diode oscillator so that the height oscillations in the film can be detected with standard FM techniques. All results reported were performed at about .1K. No systematic temperature dependence has yet to be observed.

The rotating wave modes are driven at an amplitude measured by the pickup capacitor. Swirling can be detected while driving by observing the phase of the height oscillations. After either some time, or a sweep through the resonance, the drive is turned off and the precise state of the induced persistent circulation is determined by the Doppler shift of several of the lowest resonant modes, which for the boundary

conditions in this cell correspond to a wavenumber  $k = x_m/a$  with  $x_m = 1.841, 3.054, 4.201\dots$  for the Bessel function wave solutions.

In the absence of any DC flow, the resonances associated with the azimuthal number  $m$  are ideally doubly degenerate because of the circular symmetry. For a given flow field within the circular resonator, each mode is split according to the distribution of DC flow relative the mode's AC wave field and a small geometrical component. A measured set of splittings can be analyzed to reveal a filtered knowledge of the flow field in much the same way that knowing a few of the lowest Fourier components gives you a filtered knowledge of a waveform.

### 3. NUMERICAL SIMULATION

A simple model is investigated for comparison to the experiments. Within this model, the polarization process is assumed to have reached some sort of steady state. The vortices are modeled as points that experience both a Magnus force and a frictional drag.<sup>3</sup> This simplifies the more complicated proper handling of vortices as three dimensional flow states with microscopic structural changes responding to boundary conditions. In the presence of the third sound wave, the vortices remain stationary (aside from a small distortion in shape not considered in this model) until the Magnus force applied by the instantaneous film flow speed attains the frictional drag, or

$$\rho_s K h v_c = f_{\text{drag}} \quad (2)$$

The quantum of circulation is  $K$  and the fluid density is  $\rho_s$ . Above this critical speed, vortices are allowed to move such that the friction force and Magnus force balance. The resulting vortex motion is found by solving

$$\rho_s K h \hat{z} \times (\vec{v} - \vec{v}_s) = -f_{\text{drag}} \hat{v} \quad (3)$$

for  $\vec{v}$ . The drag force is associated with the substrate and taken as opposite to the vortex motion relative to the substrate and  $\hat{z}$  is a normal to the plane of the substrate. The vortex follows an s-shaped trajectory during these portions of the wave cycle that exceed the critical speed, moving perpendicular to the flow just above threshold and picking up a parallel component with further increases.

With the linear expression for the wave velocity field, the trajectory during the opposite phases of the wave cycle would exactly cancel, resulting in no net vortex motion. Following the discussion in the introduction, we approximate the nonlinear wave flow field by the linear velocity field solution scaled by the instantaneous thickness,

$$\vec{v}(r, \phi) = C_3 \frac{\eta}{h} \left[ \frac{\frac{m\hat{\phi}}{kr} J_m(kr) \cos(m\phi - \omega t) - \hat{r} J_m'(kr) \sin(m\phi - \omega t)}{1 + \frac{\eta}{h} J_m(kr) \cos(m\phi - \omega t)} \right] \quad (4)$$

forcing zero mass flux by proportionally reducing the flow field under regions of thick portions of the film oscillations and increasing the flow under thin portions. This introduced nonlinearity now produces a net vortex displacement because of the asymmetry in the flow throughout wave cycle.

The swirled equilibrium is then taken as the distribution of vortices throughout the cell that result in no net vortex motion at any radius within the cell. This model does not address the problem of creation, but attempts to estimate what kind of vortex densities can be expected once creation is acknowledged.

#### 4. COMPARISON OF EXPERIMENT AND SIMULATION

The data in Fig. 1 show the results of a series of sweeps through the lowest two modes at increasing amplitudes. The measured height amplitudes have been converted into the wave flow field peak velocity for each mode. The  $m=2$  mode (squares) appears to swirl at a lower peak speed than the  $m=1$  mode (circles). This interpretation can be deceptive. The simulated equilibrium for peak flow speeds 10% above the critical

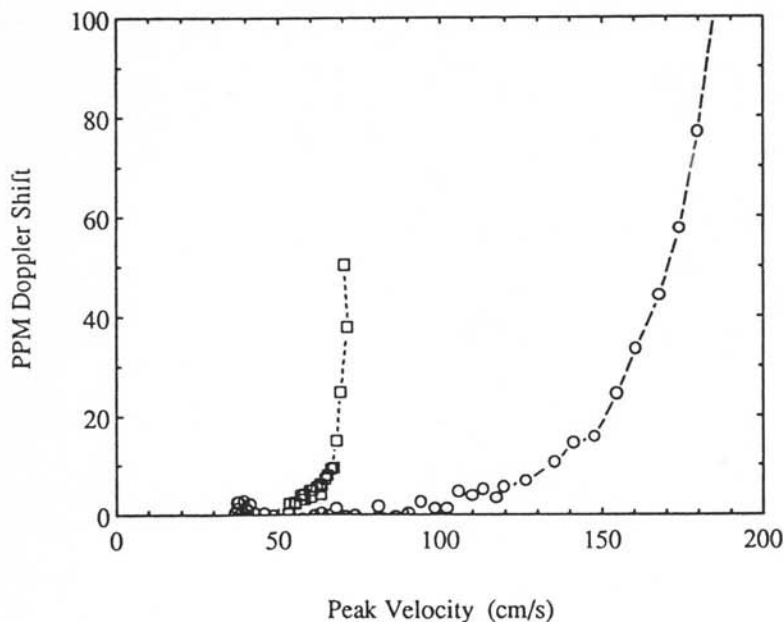


Fig. 1 Onset of the swirling in a 4.4nm film for the  $m=1$  (circles) and  $m=2$  (squares) modes. The peak velocities are deduced from the capacitive measurement of the thickness oscillations and the equations of motion.

velocity result in average splittings that are about five times larger for the  $m=2$  mode than the  $m=1$  mode. The  $m=2$  mode is apparently much more efficient at swirling.

The solid curve of Fig. 2 shows the flow field deduced experimentally for the (2,1) mode also at  $h = 4.4$  nm film. The splittings were obtained after driving at amplitudes reaching 1.6 nm (peak wave flow of 129 cm/s) over the course of 10 hours. At these large amplitudes, the (2,1) mode occasionally exhibits chaotic behavior and is difficult to maintain at a fixed amplitude. A simulated flow field produced with the same wave amplitude is shown as the dashed curve. The critical velocity used was 115 cm/s and adjusted to maximize the average Doppler splittings. Finally, the dotted curve is a classical result using the methods of Eq. (1) applied to a circular resonator.

It is apparent from the experimental results that the vortices are quite stable even in the presence of flows in the vicinity of several tens of cm/s. The density of pinning sites is on the order of  $10^4/\text{cm}^2$ , as deduced from the flow fields.

The comparisons presented in Fig. 2 demonstrate a discrepancy consistently observed between the experiment and our simulation: the experimentally determined flow fields require a much larger concentration of vorticity in the center of the

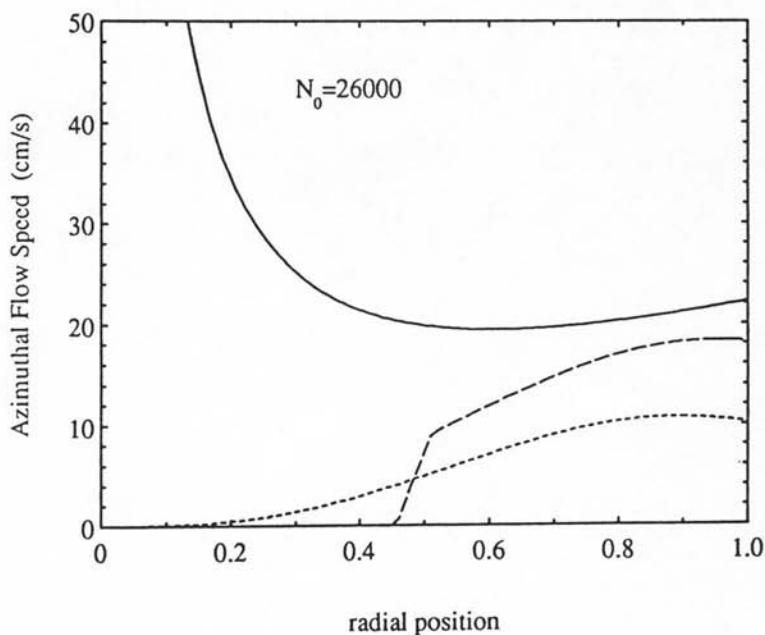


Fig. 2 Azimuthal induced flow for  $h=4.4$  nm in the  $m=2$  mode: as measured by the Doppler shifts of the lowest three modes (solid); calculated from the vortex drift simulation (dashed); and compared to a classical result (dots). The wave amplitude oscillation in all cases was 1.6 nm.  $N_0$  is the number of vortices trapped in the hole.

resonator than either the simulations or the classical results suggest. These discrepancies occur for both (1,1) and the (2,1) modes, the only modes capable of swirling the film in our resonator. In terms of the fundamental results, the splitting of the (1,1) mode, which is dominated by circulation trapped in the central hole, is consistently larger than expected by any model of vortex motion so far studied. This is especially remarkable for the (2,1) swirling where the wave flow fields are reduced to zero near the central hole, and there is little one can imagine that would contribute significantly to their being forced together in that region against their mutual repulsion. Several more complicated vortex interactions have been added to the model including a viscous type drag term and an increased pinning friction in the hole. Nothing seems to be able to overcome the absence of significant wave flow in the center of the resonator.

#### ACKNOWLEDGEMENTS

This work was supported by the National Science Foundation grant DMR-9322389 and by Wesleyan University.

#### REFERENCES

1. F. M. Ellis and L. Li, *Phys. Rev. Lett.*, **71**, 1577 (1993)
2. J. Wen and P. L. F. Liu, *J. Fluid Mech.*, **266**, 121 (1994) and references therein.
3. P. W. Adams and W. I. Glaberson, *Phys. Rev.*, **B35**, 4633 (1987)